

ITA's LOW SPEED WIND TUNNEL: CALIBRATION OF THE TEST SECTION FLOW

Marcelo Assato

Empresa Brasileira de Aeronáutica – São José dos Campos – SP- 12227-901

e-mail: assato@ita.br

Roberto M Girardi

Instituto Tecnológico de Aeronáutica – São José dos Campos – SP- 12228-900

e-mail: girardi@ita.br

Nide G C R Fico Jr

Instituto Tecnológico de Aeronáutica – São José dos Campos – SP- 12228-900

e-mail: nide@ita.br

Abstract. ITA, EMBRAER and FAPESP teamed up in a Technological Innovation Project to develop new experimental techniques to be used in the development of new EMBRAER products. As a part of this effort, a low-speed wind tunnel was designed and built at ITA. During the last months this tunnel has been under calibration. The test section turbulence level was measured as well as flow uniformity. This work presents the experimental techniques used as well as results of the test section

Keywords. wind tunnel, subsonic regime, calibration, turbulence

1. Introduction

ITA's new wind tunnel is part of a greater project of Technological Innovation (PITE) whose main objective is to increment the productivity and reliability of aerodynamic testing. This new wind tunnel is the answer to the long term need of an equipment which allows aerodynamic testing with low operating cost, as well as, low cost for the experimental apparatus implementation (complex models manufacturing can be a very expensive activity). The requirements above can be satisfied with a 1.0 x 1.28 m test section, where a flow with, at least, 70 m/s must be established, in order to reach, at least, a Reynolds number of 10^6 . Previous work describes the early stages of the project which includes the influence of external winds on the tunnel intake was evaluated (Assato et al, 2003) and the tunnel contraction was numerically simulated to ensure good test section flow quality (Mattos et al, 2003) as well as the tunnel design and initial calibration data (Assato et al, 2004). The original tunnel concept is shown in Fig. 1. Notice that from the entrance nozzle up to section the tunnel lies inside Prof. K.W. Feng Aeronautical Engineering Laboratory. The diffusers, the fan and the tunnel discharge to the atmosphere are outside the building.

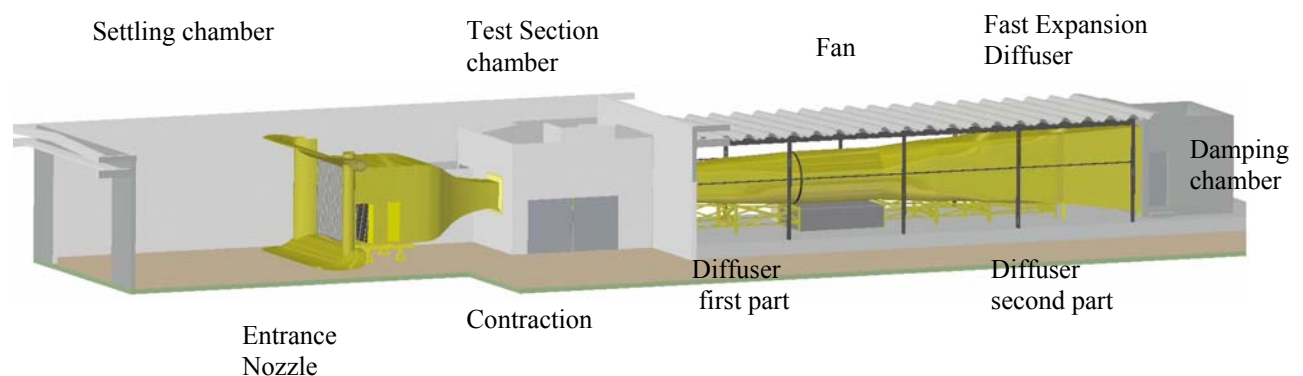


Figure 1. View of ITA's low-speed wind tunnel inside Prof. Feng Aeronautical Engineering Laboratory.

ITA's wind tunnel started operation on the first semester of 2003 with a series of preliminary experiments to calibrate the test section flow. During that stage of the work it was found a very high turbulence level at the test section (Assato et al. 2004). One of the causes for that undesirable result is the free shear layer originated at the laboratory's door. In order to eliminate it an additional tunnel element was built. The new air intake is shown in Fig. 2. From Fig. 2 it is clear that this new air intake eliminates not only the above mentioned free shear layer but also makes the incoming

air symmetrical with respect to the tunnel center line. Notice that the original air inlet section is much closer to the wall at its right side.

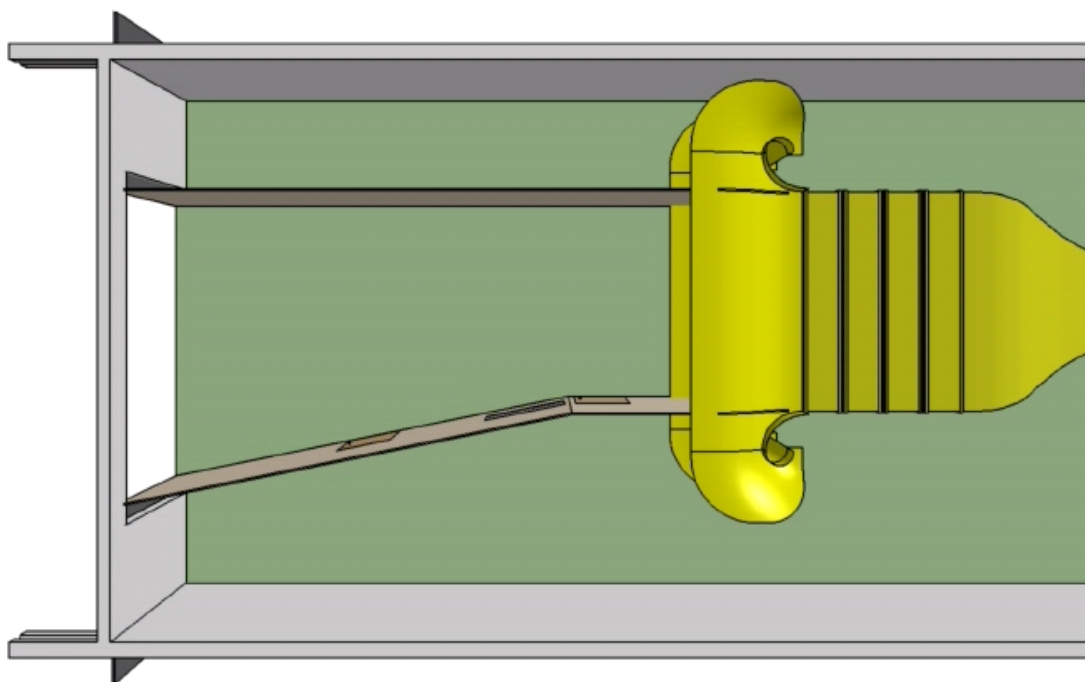


Figure 2. Top view of the tunnel inlet chamber.

After the calibration phase, which is now under way, two research programs will be implemented to reach the following objectives: (i) Experimental methodology development to minimize the three-dimensional flow observed in two-dimensional airfoil models at high angles of attack. This problem occurs due to the interaction between the airfoil extremities and the tunnel wall boundary-layer flow and cause great uncertainty in the measurements of the airfoil maximum lift coefficient, $c_{l_{max}}$. (ii) Development of a methodology for estimating a wing's $C_{L_{max}}$, once the airfoil's $c_{l_{max}}$ is known. In order to accomplish this objective a set of experiments will be conducted to understand the separated flow evolution, at the upper surface of a wing, while the angle of attack is incremented up to the wing stall. It is worth to mention that these two research programs were proposed by the EMBRAER personnel to solve important practical problems.

The main objective of the present paper is to report the calibration results of ITA's low-speed wind tunnel.

2. Test Section Flow

In this section results of the test section flow uniformity, velocity profiles within the tunnel boundary layer along the test-section walls as well as the turbulence level at the test section are presented.

2.1. Test-section flow uniformity

To measure the tunnel flow uniformity two pressure transducers were used: 1psi and 1 mbar. One of them, connected to a Pitot-static tube located at the test section, shown in Fig 3, is responsible for the data acquisition at the test section. No fence was used, as seen in Fig 3, because the objective here is to map the test section flow. The other transducer measures the dynamic pressure given by the rings located upstream of the test section, see Fig 4. The test section flow temperature was monitored by a thermocouple located at the stilling chamber. The noise induced by the frequency inverter that controls the fan was eliminated by a 1.0 KHz low-pass filter.

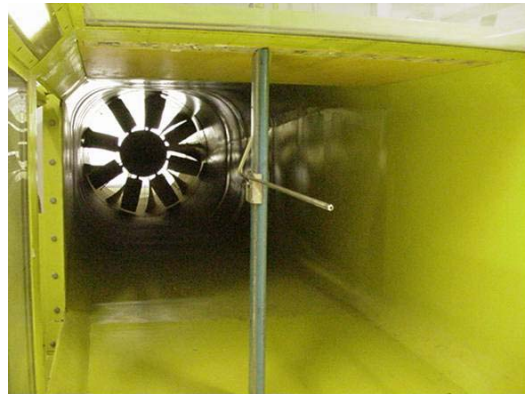


Figure 3. Pitot-static tube mounted within the test section.

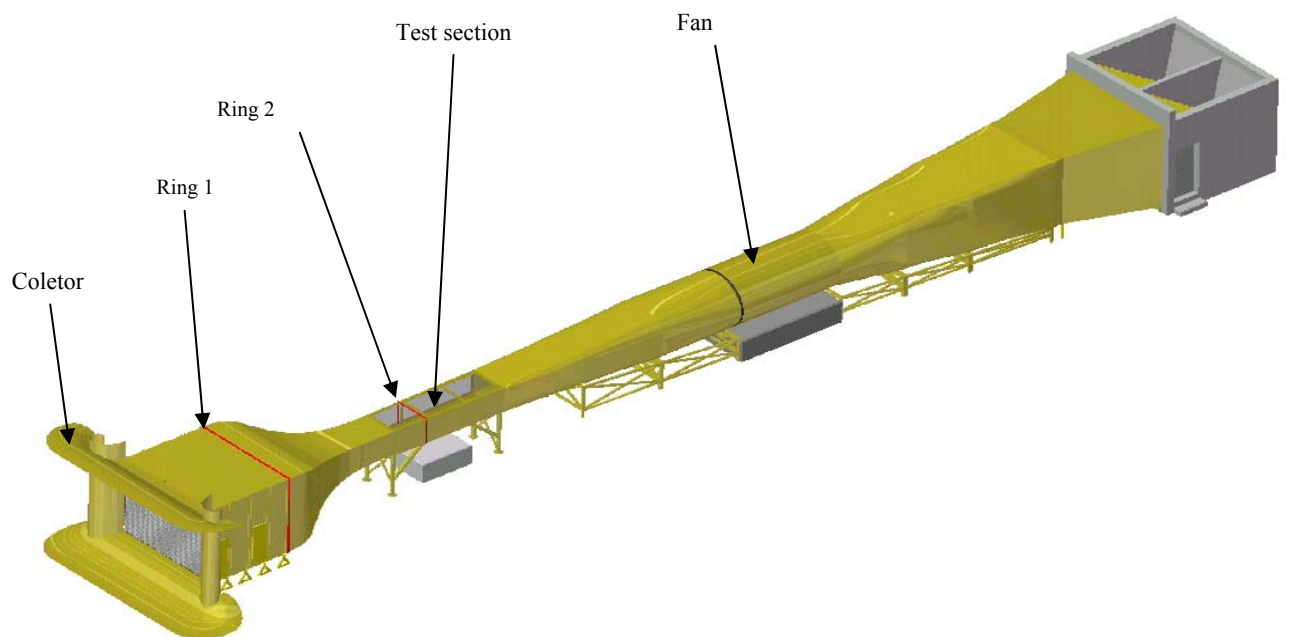


Figure 4. Tunnel rings locations

The tunnel test section is four meters long. The flow uniformity measurements were made at the mid-cross section, that is, two meters from the test section entrance. Two different fan rotations were 400 rpm and 800 rpm. The Pitot tube, shown in Fig. 3, can be traversed, in the plane of interest, by 10-cm increments to cover the whole cross section. The Pitot mounting proved to be very rigid. The flow uniformity was calculated by

$$\eta = \frac{P_{t(Pitot)}(y, h) - P_{t(ring)}}{q_{dyn(rings)}}, \quad (1)$$

where $p_{t(Pitot)}(y, h)$ is the total pressure measured by the Pitot-static tube, $p_{t(ring)}$ is the total pressure measured at the stilling chamber by ring 1, and $q_{dyn(rings)}$ is the dynamic pressure obtained with the aid of rings one and two. The difference between the two dynamic pressures, $p_{t(Pitot)}(y, h) - p_{t(ring)}$, is measured by a 1-mbar transducer.

Taking the mean value of the flow uniformity parameter, $\bar{\eta}$, as the reference value one can calculate the flow uniformity distribution, ξ . Thus,

$$\xi = \eta - \bar{\eta} \tag{2}$$

Figure 5 displays the flow uniformity, ξ , for the fan rotations investigated, 400rpm and 800 rpm. These rotations correspond to dynamic pressures equal to 77 mmH₂O e 310 mmH₂O, respectively. It can be observed that the flow uniformity, deviates $\pm 0.25\%$ from its mean value in both cases.

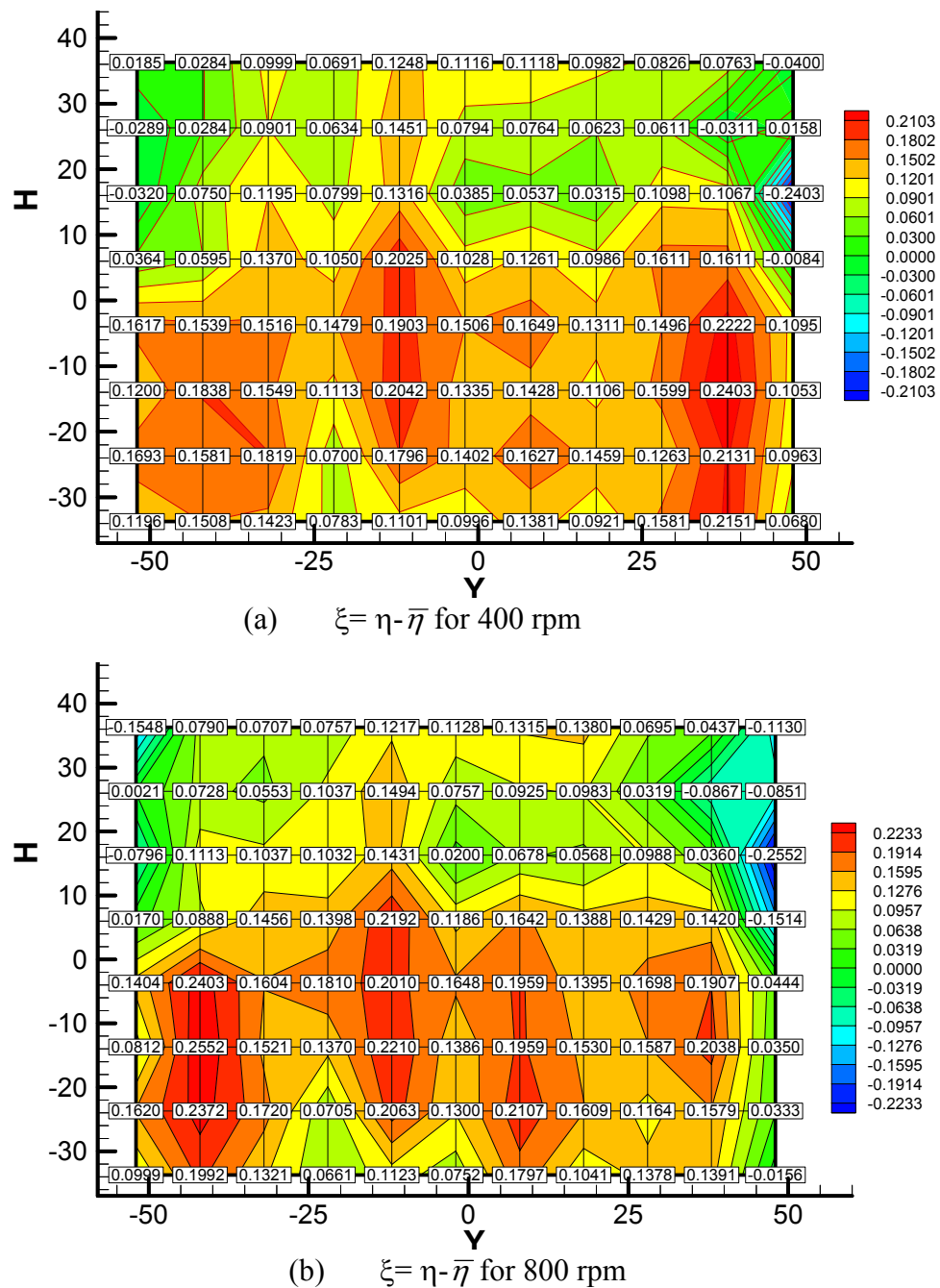


Figure 5. Flow uniformity distribution at a cross-plane located at the test section mid length.

The results indicate that the flow volume at test section lower half is greater than at the upper half. This may be a consequence of the door asymmetry. Further investigation is needed to clarify this point.

2.2 Velocity Profiles

The velocity profiles as well as the turbulence intensity at the lateral walls, at the tunnel floor and at the tunnel ceiling for several fan rotations are presented next. A one component hot-wire anemometer was used to sweep the boundary layer, see Fig. 6. As done for the flow uniformity measurements, the hot-wire input to the data acquisition system was filtered to avoid noise introduced by the frequency inverter that controls the fan speed.

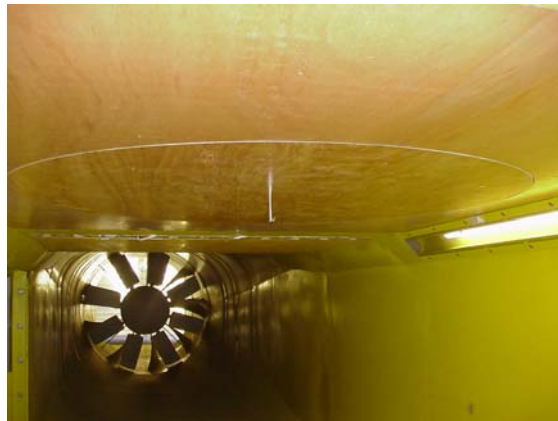


Figure 6. Hot-wire anemometer mounted at the test section

Figure 7 (a) displays the non-dimensional velocity profile versus the distance from the wall for three fans rotations: 400 rpm, 600 rpm and 750 rpm. These correspond to a non-disturbed dynamic pressure, q_{∞} , equal to 100, 235 and 355 mmH₂O. Figure 6 (b) shows the turbulence intensity as function of the distance from the wall for the same fans rotations.

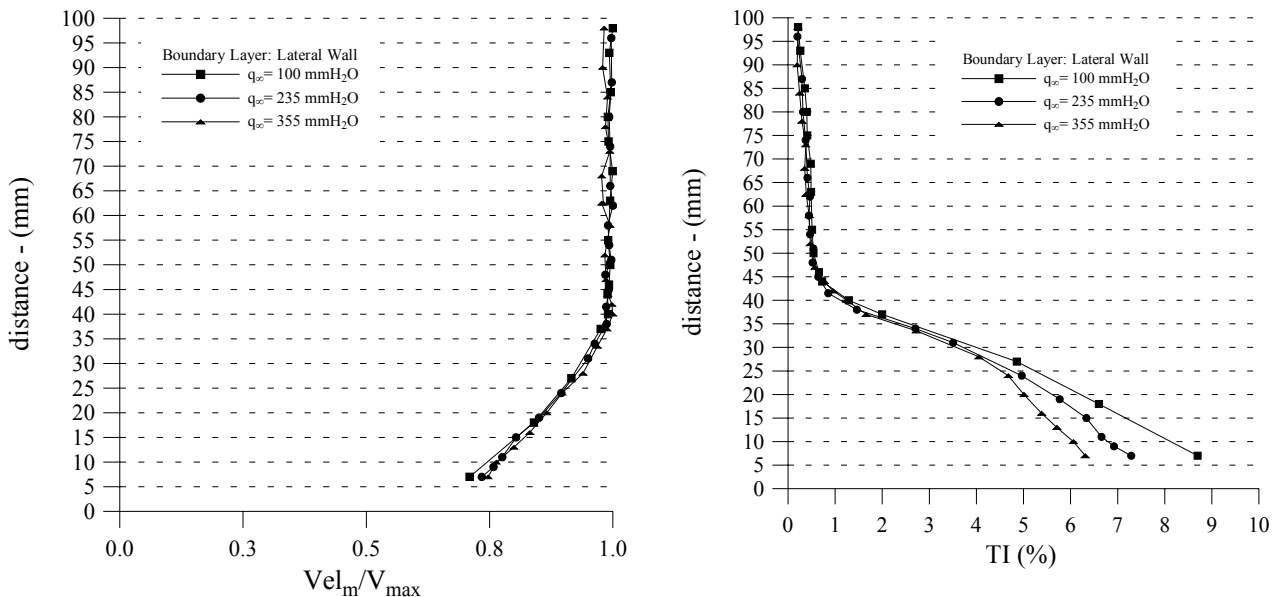


Figure 7. Velocity profiles and turbulence intensity at the tunnel lateral wall for three different fan rotations.

For the tunnel floor both the non-dimensional velocity profile as well as the turbulence intensity were measured for the following fan rotations: 400 rpm, 500 rpm, 600 rpm, 700 rpm and 800 rpm. In Fig. 8 the results for the maximum rotation investigated, namely 800 rpm, are shown.

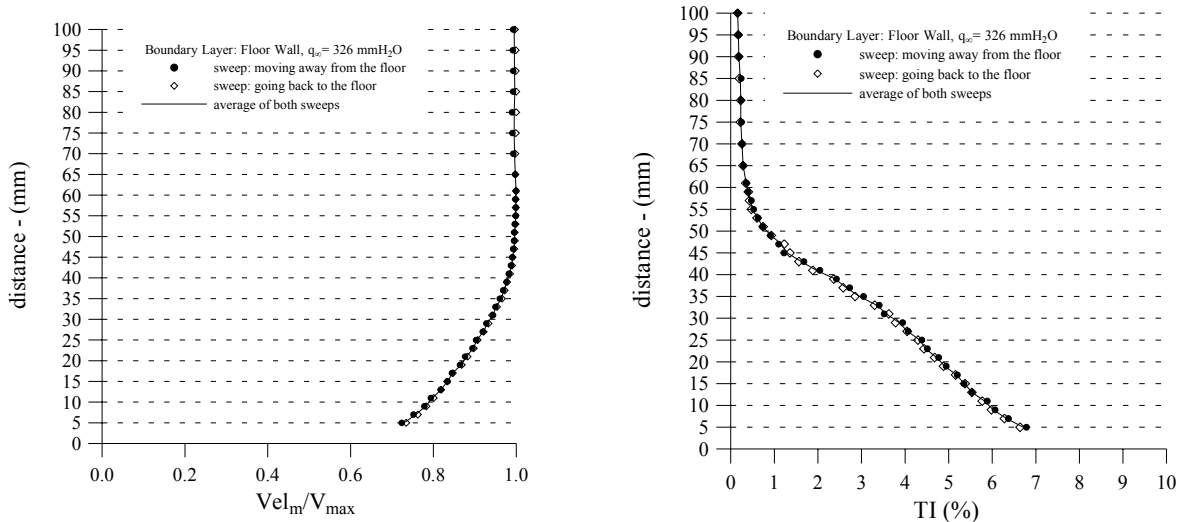


Figure 8. Velocity profiles and turbulence intensity at the tunnel floor for 800 rpm.

Finally results for the tunnel ceiling are presented. The non-dimensional velocity and the turbulence intensity profiles were measured for the same fan rotations used for the investigation at the tunnel floor, ranging from 400 rpm to 800 rpm with 100-rpm increments. The results for 800 rpm are presented in Fig 9.

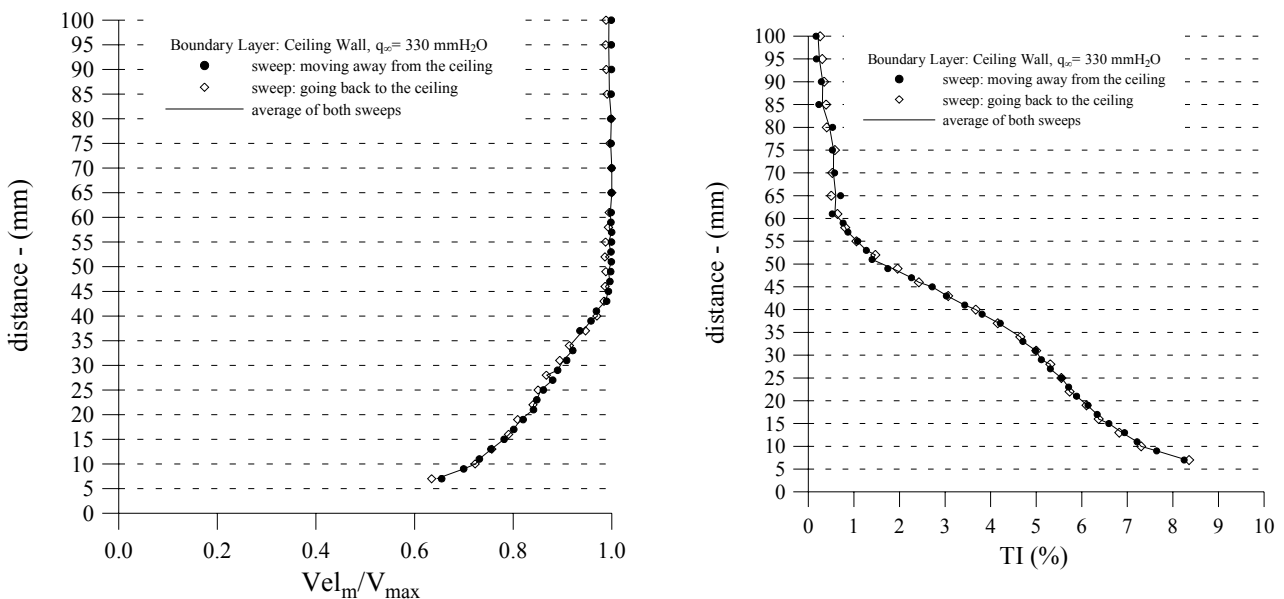


Figure 9. Velocity profiles and turbulence intensity at the tunnel ceiling for 800 rpm.

The profiles for the tunnel floor as well as for the tunnel ceiling were obtained as average of a sweep away from the tunnel boundary followed by a sweep towards the wall in order to minimize the experimental error.

The data presented in Figs. 7 to 9 was used to calculate three important boundary layer parameters, namely the boundary layer thickness, δ , the displacement thickness, δ^* , and the momentum thickness, θ . The results are in Table 1. Looking at the numbers, one can see that the, especially at the floor and at the tunnel ceiling, the boundary layers developed quite similarly. Thus the contraction is yielding a uniformly distributed flow at the test section entrance. This is a good indication regarding the test section flow quality.

Table 1 Boundary-layer parameters at the test section mid cross-section

Dynamic pressure (mmH ₂ O)	Boundary layer thickness δ (cm)			Displacement thickness δ^* (cm)			Momentum thickness θ (cm)		
	Floor Wall	Ceiling wall	Lateral wall	Floor Wall	Ceiling wall	Lateral wall	Floor Wall	Ceiling wall	Lateral wall
88	4.4	4.5	----	0.83	0.96	----	0.40	0.48	----
100	----	----	3.9	----	----	0.91	----	----	0.45
130	4.5	4.4	----	0.88	0.88	----	0.43	0.42	----
188	4.4	4.3	----	0.82	0.97	----	0.39	0.49	----
236	4.4	4.5	3.8	0.77	0.86	0.85	0.39	0.41	0.40
330	4.2	4.3	----	0.72	0.98	----	0.38	0.48	----
355	----	----	3.45	----	----	0.73	----	----	0.31

2.3 Turbulence Level

The last results to be presented here are related to the turbulence level at the mid cross section plane of the test section. ITA's Low Speed Wind Tunnel was designed to have a very low turbulence intensity level, TI, at the test section. The turbulence intensity is given by

$$TI = \frac{U_{rms}}{U_{mean}} \times 100, \quad (3)$$

where

$$U_{mean} = \frac{1}{N} \sum_{i=1}^N U_i \quad \text{and} \quad U_{rms} = \left(\frac{1}{N-1} \sum_{i=1}^N (U_i - U_{mean})^2 \right)^{0.5} \quad (4)$$

The design goal was TI = 0.05% a very ambitious number. As usual care was taken to free the experimental data of the noise associated to the frequency inverter. This influence was actually quantified but the authors refrain to shown these results here due to lack of space. Also, in order to increase the accuracy, the hot-wire anemometer was calibrated for different velocity ranges. The data acquisition system was set to a sample rate of 30 kHz and for each measurement 300,000 readings were made. A high pass filter was set at 3.0 Hz and a low pass filter was set at 10 kHz. The signal gain was equal to 10. The final value of the turbulence intensity at each point investigated was obtained after 20 measurements. The hot-wire probe placed inside the test section is shown in Fig. 10.



Figure 10. Hot-wire anemometer probe inside the test section.

As stated in the introduction the tunnel air intake has been modified after analyzing the first calibration results related to the turbulence level at the test section. As one can be seen in Fig 11, the original tunnel air intake was asymmetric in respect to the laboratory's wall. Further the free shear layer originated at the building's door was directly affecting the tunnel's flow. The new air intake, also shown in Fig 11 overcome both of these problems and lowered significantly the TI at the test section.

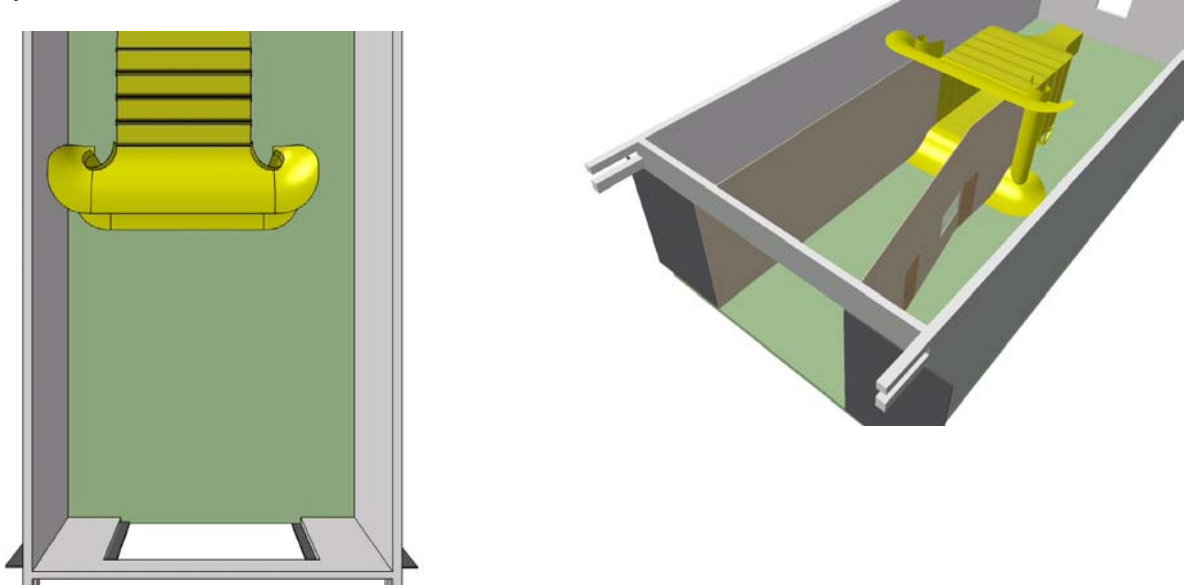


Figure 11. Comparison of the original tunnel intake, at left, with the new inlet chamber at right

Figure 12 shows the influence of the high-pass filter on the turbulence intensity results. It is almost impossible to obtain the desired the 0.05% desired at the test section if no filter is used. There are many sources of noise, such as the frequency inverter.

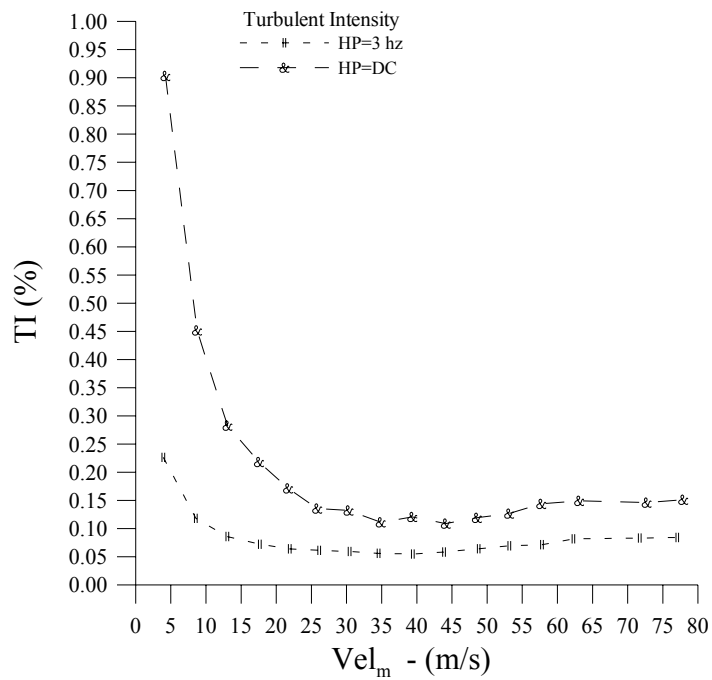


Figure 12. Influence of the filter on the turbulence intensity for different velocities at the test section

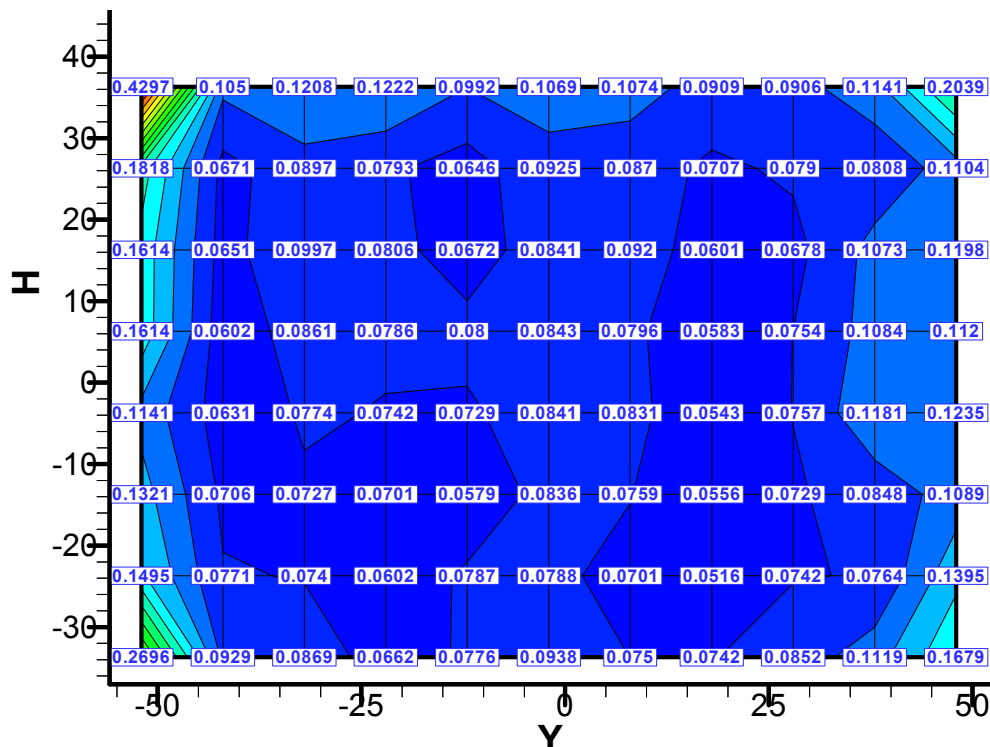


Figure 13. Turbulence intensity at the test section with new inlet chamber

Figure 13 shows the turbulence intensity distribution at the test section. It can be seen that near the walls the value of this parameter is higher than at the test section core due to the boundary layer influence. One also can observe that nowhere, at this particular cross section, located exactly at its mid-length $TI = 0.05\%$ was achieved. However, it must be stressed that a very good improvement was obtained when the present results are compared with the ones before the inlet chamber was constructed (Assato et al, 2004)

3. Conclusion

This work reports some calibration results for ITA's Low-speed Wind Tunnel. A very detailed and careful experimental study was undertaken. Much more than what has been shown herein has been done. During this calibration phase a lot has been learned related not only to the actual tunnel flow quality but also, and more important, many experimental procedures have been developed. The tunnel flow quality is adequate to the research work that needs to be tackled in the near future, although some small improvements may have to be done to obtain a very low turbulence level at the test section.

4. Acknowledgement

The authors would like to acknowledge Fundação de Amparo a Pesquisa do Estado de São Paulo (FAPESP), for partially supporting the construction of ITA's wind tunnel under grant FAPESP 00/13769-0. We also like to thank EMBRAER for supporting the modifications required to the infra-structure of the Prof. K.W. Feng Aeronautical

5. References

- Assato, M., Fico Jr, N.G.C.R and Girardi, R.M., 2003, "Experimental Study of the Turbulence Level at the Intake of an Open Circuit Wind Tunnel", Paper AIAA-2003-3948, 21st AIAA - Applied Aerodynamics Conference, 23 - 26 Jun, Session 86: Wind Tunnel Aerodynamics and Experimental Studies II, Orlando, Florida, USA.
- Assato, M., Girardi, R. M., Fico, Jr, N.G.C.R., Mello, O. A. F. and Komatsu, P., 2004, "Research Wind Tunnel of the Aeronautical Institute of Technology: Conceptual Design and Calibration, AIAA Paper 2004-0724, 42nd Aerospace Sciences Meeting, 05-08 Jan., Reno, Nevada.
- Mattos, B., Fico Jr, N.G.C.R and Girardi, R.M., 2003, "Design of the Contraction of ITA's Research Wind Tunnel Using CFD Tools", Paper AIAA-2003-3949, 21st AIAA - Applied Aerodynamics Conference, 23 - 26 Jun, Session 86: Wind Tunnel Aerodynamics and Experimental Studies II, Orlando, Florida, USA.